A two-regime analysis of the COVID-19 vaccine distribution process

Sharika J. Hegde and Hani Mahmassani
Transportation Center, Northwestern University, Evanston, Illinois, USA, and
Karen Smilowitz
Department of Industrial Engineering and Management Sciences, Northwestern University, Evanston, Illinois, USA

Abstract

Purpose – The purpose of this paper is to develop a framework to evaluate and assess the performance of the COVID-19 vaccine distribution process that is sensitive to the unique supply-side and demand-side constraints exhibited in the US vaccine rollout.

Design/methodology/approach – A queuing framework that operates under two distinct regimes is formulated to analyze service rates that represent system capacity to vaccinate (under the first regime) and hesitancy-induced throughput (under the second regime). These supply- and hesitancy-constrained regimes form the focus of the present paper, as the former reflects the inherent ability of the nation in its various jurisdictions to mobilize, whereas the latter reflects a critical area for public policy to protect the population's overall health and safety.

Findings – The two-regime framework analysis provides insights into the capacity to vaccinate and hesitancy-constrained demand, which is found to vary across the country primarily by politics and region. The framework also allows analysis of the end-to-end supply chain, where it is found that the ability to vaccinate was likely constrained by last-mile administration issues, rather than the capacity of the manufacturing and transportation steps of the supply chain.

Originality/value – This study presents a new framework to consider end-to-end supply chains as dynamic systems that exhibit different regimes because of unique supply- and demand-side characteristics and estimate rollout capacity and underlying determinants at the national, state and county levels.

Keywords COVID-19 vaccines, Logistics, Supply chain, Queueing system, Multi-regime models, Vaccine hesitancy

Paper type Research paper

1. Introduction

The World Health Organization declared the COVID-19 viral outbreak a global pandemic in March of 2020. It took under a year for vaccines to be developed, for several to receive authorization for emergency use and for rollouts to begin around the world. The deployment of COVID-19 vaccines represents a unique man-made experiment in extreme logistics. An operation of such scale, magnitude and urgency requires a complex, global network of transport and logistics facilities and services. The logistical processes must move not only vaccines but ancillary equipment such as syringes and dry ice for refrigeration to enable vaccination at desired rates within its limited shelf life. They must also mobilize last-mile distribution and local labor-intensive administration processes. In addition to the supply-side constraints in manufacturing, distribution and administration, the COVID-19 vaccines face demand-side considerations that determine the take-up rate as people in the USA, and around the world must voluntarily accept the offered vaccines. Initially, the demand for vaccines well outpaced the supply in the USA and around the world, but as the rollout progressed, a significant population of unvaccinated people was left questioning the safety and efficacy of the vaccines, likely due to widespread misinformation (Loomba *et al.*, 2021). Both supply and demand-side constraints have affected the USA' ability to quickly reach high vaccination rates, which has left open the possibility for new strains to emerge, potentially requiring boosters (Macmillan, 2021), and ultimately extending the COVID-19 pandemic's disruption to daily life.

As of October 2021, over 213 million people received at least one vaccine dose, and over 185 million people were fully vaccinated by either the single-dose vaccine made by Johnson & Johnson or by one of the two-dose series made by Moderna and Pfizer-BioNTech in the USA. This constitutes 64% and 55% of the US population, respectively. While the first doses were

The current issue and full text archive of this journal is available on Emerald Insight at: **https://www.emerald.com/insight/2042-6747.htm**

Journal of Humanitarian Logistics and Supply Chain Management
13/2 (2023) 111–124
Emerald Publishing Limited [ISSN 2042-6747]
[DOI 10.1108/JHLSCM-10-2021-0106]

This material is based upon work supported by a National Science Foundation grant to Dr Hani Mahmassani and Dr Karen Smilowitz titled "RAPID: Tracking and Deconstructing COVID-19 Vaccine Distribution as an Extreme Logistics Event."

Received 8 October 2021
Revised 16 August 2022
Accepted 8 January 2023

administered in the USA in December of 2020, vaccine production did not significantly ramp up until March 2021 when 71 million doses were distributed within the month, more than twice the 33 million doses delivered across the USA in February 2021. The peak 7-day rolling average of the daily vaccination rate was on April 13, 2021, when 3.38 million new doses were administered in the USA. Since the Spring of 2021, however, this rate has dramatically reduced with just over 500,000 new doses administered on July 11th across the nation. Between August and September of 2021, the vaccination rate has once again increased, likely in response to the spread of the highly contagious Delta variant across the country and the full approval of the Pfizer vaccine by the FDA on August 23.

These observed trends in vaccination rates indicate aggregate changes in the relationship between the supply and demand for vaccines in the USA. Based on observations in the USA, the vaccination rate can be characterized in multiple regimes, as it initially exhibits a supply-constrained behavior where there is extreme demand to get vaccinated, followed by a hesitancy-constrained behavior once there is a sufficient supply of vaccines. In this paper, vaccination rates and administered doses are tracked and compared at a national, state and county level and analyzed through a queuing framework to understand how the supply-constrained capacity to vaccinate and the hesitancy-constrained behavior of people to seek vaccination vary across the country. Analysis using this multi-regime framework allows us to characterize the COVID-19 vaccine rollout and develop principles for the robust design and resilient operation of future extreme logistics deployments, while also recognizing how different factors affect vaccination rates.

The paper's main contributions consist of the following:

- formulating a two-regime characterization of the vaccine deployment as an extreme logistics process;
- quantifying the practical capacity of such deployments at a national level;
- characterizing the factors that determine an area's capacity to vaccinate its population and its variability across different spatial units (county and state level); and
- providing insight into the determinants of vaccine hesitancy as a limiting factor on the ability to fight future pandemics.

While the framework's applicability is general, the specific vaccination and hesitancy rate models developed are based on US data.

The paper is organized as follows. Section 2 presents a review of relevant studies, followed in Section 3 by a description of the data that forms the basis of the analysis presented in this paper. The conceptual framework and overall methodology are described in Section 4. Estimation of vaccination capacity and vaccine hesitancy rates, respectively, are conducted using multiple regression models that relate these rates to socio-demographic, economic and other indicators at the county level; the models and associated results are presented in Section 5. Finally, Section 6 contains a discussion of the two-regime model presented and conclusions regarding the logistical preparations for future mass deployments.

2. Literature review

Queuing theory is used to mathematically understand how people or objects move through systems. Basic queuing theory refers to objects, servers or restrictions and queues or reservoirs, where the system is defined by the rate of arrival into the queue, the amount of time required for service and the number of servers available (Newell, 2013). Fundamentally, when the arrival rate is low relative to the capacity of the server(s), the waiting times are low and the queue length is short. However, if the arrival rate is relatively high, the waiting times and queue lengths are longer. Queue lengths fluctuate and may build up over time due to stochasticity in both the arrival and service processes, even when service rates exceed arrival rates on average (Kleinrock, 1975). The performance of queueing systems can be assessed through the time spent waiting in the queue, the time required for service, the proportion of time servers are used, system throughput, queue length, etc. (Hall, 1991). Graphically, queuing systems can be represented through cumulative arrival and departure curves where the queue length is extracted from the vertical distance between the curves, and the waiting time in the system is represented by the horizontal distance between the curves. Extracting individual or object-level statistics, however, requires an understanding of the service discipline, which may be other than "First-Come-First-Served".

Application areas of queuing theory are broad, aiding operations research in service industries, supply chain management and transportation, among other fields. For example, queuing frameworks are often used in traffic flow theory to understand system performance at bottlenecks by tracking cumulative vehicle arrivals and departures over time (Newell, 1993). While knowledge of the arrival rate parameter into the system is often considered central to a queuing analysis, methods for inferring these statistics empirically are also prevalent. Larson's Queue Inference Engine considers only the recorded timestamp data for when automated teller machine service starts and stops and provides a method to estimate customer waiting time from the digital transactional data (Larson, 1990). Although classical queuing theory primarily considers the stochastic fluctuations from a stationary state, generalizations of queuing approaches can model nonlinear interactions in a continuous fluid interpretation of supply chains to capture behaviors such as the bull-whip effect of inventory increases up a supply chain (Helbing and Lämmer, 2005).

In medical and health-care settings, queuing analysis can be used to analyze inefficiencies within systems through resource allocation and scheduling problems, ultimately improving measures such as patient waiting time, prescription fill time, hospital bed utilization and staff and facility management (C and Appa Iyer, 2013). Many of these studies focus on documenting the distribution of experienced waiting times and utilization rates and identifying facility-specific bottlenecks in the health-care systems that can be addressed (C and Appa Iyer, 2013). Typically in these applications, waiting time problems are considered with an assumed Poisson arrivals process and a negative exponential service time distribution (Kapadia *et al.*, 1985). Queuing applications in health care often tackle supply-constrained problems.

In addition to applications in resource utilization and patient experience, health-care supply chains can also be viewed within a queuing framework. Vaccine supply chains can broadly be categorized into four main segments: the national sourcing of vaccines, vaccine storage, vaccine transport and vaccine administration. Vaccine distribution has long been a challenging task in low-income countries (De Boeck *et al.*, 2020), however even in the USA, the distribution of vaccines has experienced many of the uncertainties seen in other supply chains. The supply of tetanus and diphtheria vaccines for children, for example, exhibited extreme shortages in late 2000 due to two manufacturers reducing production (CDC, 2001). As a result, thousands of children were not immunized on time, heightening the risk of epidemic outbreaks and motivating the development of stochastic inventory models to establish adequate vaccine supply during production interruptions (Jacobson *et al.*, 2006). However, the vaccines supply chain also exhibits some unique characteristics as it is often characterized by a "misalignment of objectives and decentralized decision making" as manufacturers are not always developing vaccines themselves, and those receiving vaccines are not usually paying for the product (Duijzer, van Jaarsveld and Dekker, 2018). Additionally, those who pay for vaccines are typically not-for-profit organizations, which often leads to supply chain asymmetries and a need for better coordination (Herlin and Pazirandeh, 2012).

Particularly in the context of the COVID-19 pandemic, the intense level of demand and the severe shortage of supply in the early months of the rollout proved an extreme logistics event for even the largest economies. Vaccines were originally allocated to states by the federal government according to the 18+ population size in the states (Singer, 2021). States may then allocate doses across their jurisdictions. As of May 10, 2021, however, many have found the vaccine supply sufficient, allowing providers to directly order doses (Texas DSHS, 2021). From end-to-end, the vaccine rollout faces a variety of challenges related to manufacturing, cold chains, last-mile delivery and hesitancy-constrained demand (Alam *et al.*, 2021). Once the vaccines are sourced from the limited number of manufacturers, initial transportation constraints not only include the timely delivery of first-generation vaccines and ancillary equipment in an ultra-cold chain, but they must also stop cargo from being stolen and prevent any disruptions that could threaten the viability of vaccine doses (Forman *et al.*, 2021). At the end of the supply chain, the manpower to administer doses and hesitancy may have constrained vaccination rates. Vaccination hesitancy is driven by both personal concerns and misinformation around the speed at which the vaccines were developed as well as the suspicions about the varying requirements and regulatory advice across governments and agencies (Forman *et al.*, 2021). Similar effects are the result of anti-vaccination sentiment driven by the rapid spread of misinformation on social media (Roozenbeek *et al.*, 2020).

As discussed, the supply chain and administration of COVID-19 vaccines face unique challenges on both the supply and demand sides. To fully characterize the end-to-end vaccine pipeline, it is necessary to consider how the dynamics of the system have evolved over the period between December 2020 and September 2021.

3. Data sources and preparation

This study focuses on the USA vaccine rollout, primarily due to data availability, including contextual data directly from major players in the rollout process. The two-regime framework presented in the paper is the result of tracking and analyzing vaccination metrics over time at various spatial levels in the USA. Data for this study is obtained from a Web portal dashboard developed by the authors to track vaccine logistics. This dashboard pulls data daily from the US Centers for Disease Control and Prevention, along with various state departments of health, to augment missing data from the centers for disease control and prevention (CDC) portal. In addition to these data sources, the dashboard pulls data from the U.S. Census Bureau's statistical regions and divisions (U.S. Census Bureau, 1984) and county-level demographic data (U. S. Census Bureau, 2019), 2020 presidential election results (MIT Election Data + Science Lab, 2021) and urbanization level (USDA ERS, 2013) to characterize vaccination rates across the country.

An important part of our data collection effort is to contextualize the vaccine logistics process, understand the flows of vaccine and ancillary products and correctly interpret the information provided through the various official channels. Accordingly, interviews were conducted with representatives of the unit originally referred to as "Operation Warp Speed", representatives of the major carriers involved in various stages of the vaccine supply chain, health officials at the state, county and city levels, and entities physically performing vaccination such as pharmacies and hospitals. The main picture that emerges from these interviews is that the delivery of vaccines and ancillary products from the manufacturers and their warehouses to the designated locations in each state essentially flowed accordingly to plan. All players in that supply chain generally lived up to expectations and managed to complete deliveries on a weekly schedule; disruptions occurred only for one week due to severe inclement weather in parts of the midwestern USA. In other words, all entities involved in this process agreed that the planning that went into this operation resulted in a smooth and generally predictable delivery process from sources to intended destinations. The significance of this information is in helping interpret where the bottlenecks existed in the process. Throughout the distribution process, as shown in the graphs in the next section, the quantities that the CDC indicated had been delivered to the various states were consistently above the ground vaccination rate. This fact is critical to the two-regime interpretation advanced in this paper, as described in the next section.

4. Methodology

4.1 Motivation and general observations

The COVID-19 vaccine rollout in the USA exhibited multiple phases. Initially, there is a buildup phase when supply ramps up, starting in December 2020 and continuing through the beginning of 2021. The ramp-up process encompasses both production and distribution processes and local agencies' abilities to vaccinate residents, as various last-mile models are pursued in various parts of the country, in different parts of the same state and, in some instances, the same county. A supply-constrained phase follows where the demand for doses exceeds

the capacity to administer. In this regime, the system experiences extreme demand but is limited by the ability to vaccinate. In a queuing framework, the supply-constrained regime can be interpreted as the vaccination capacity of the system. Following this regime, the system exhibits a hesitancy-constrained vaccination rate, where the vaccination rate in effect reflects the behavior of people to seek vaccination and is therefore no longer reflecting the system's capacity to provide this service, instead depicting demand under hesitancy.

Figure 1 depicts the average daily number of doses administered for the previous 7-days across the USA from December 2020 to September 2021. Various daily events are labeled.

As shown in Figure 1, the daily dose administration rate increases steadily from December of 2020 until mid-April 2021. The peak 7-day average vaccination rate is experienced on April 13, when over three million doses are administered across the country. The daily number of doses administered is receptive to transportation delays, as seen by the dip in administered doses following the winter storm delays in February (Nirappil *et al.*, 2021). Additionally, the daily administration has steadily increased from July onwards, likely in response to guidance from the CDC regarding the Delta variant.

While the national vaccine administration follows the trend depicted in Figure 1, actual vaccination rates vary depending on local conditions. Figure 2 depicts the daily vaccination rate across counties. To account for differences in county size, the county daily population percent vaccinated is plotted over time. Counties are aggregated based on region, politics and urbanization, where data points represent the average daily rates across counties in each aggregation group. Regional aggregation groups are determined by the U.S. Census statistical regions. Politically, counties are labeled based on the 2020 Presidential Election results, where counties that recorded more than 60% of their votes for the Democratic or Republican party nominee are labeled, respectively, and those without the threshold of votes are "Center." Finally, to capture urbanization, counties are labeled according to the 2013 Urban Influence Code, which is developed by the US Department of Agriculture's Economic Research Service. The 2013 Urban Influence Code ranges from 1 to 12, where 1 indicates a county within a large metro area of 1+ million residents and a score of 12 indicates counties not adjacent to any metro/micro area and do not contain towns of at least 2,500 residents.

Evident in Figure 2 are clear differences by region, politics and urbanization. At peak vaccination, counties in the Northeast can vaccinate close to 0.7% of their population per day while counties in the South are averaging just under 0.3% of their populations. Democratic-leaning counties and urban counties generally vaccinated at higher rates. It is of interest that county-groups with lower peak vaccination rates, such as southern, Republican-leaning and rural counties, exhibit their peaks significantly earlier than other county-groups.

4.2 Conceptual framework

The preliminary plots above show distinctions in vaccination rates across the country. Fully analyzing the end-to-end performance of the vaccine supply chain requires understanding how and why vaccination rates vary. This conceptual two-regime framework allows analysis of supply chain performance both in breadth and depth. Due to data availability, the conceptual framework is applied at the national, state and county levels in the USA.

When considering the adoption of vaccines, a diffusion curve where agents are individually making adoption decisions is expected. Diffusion curves for the adoption of technology, for example, often show an adoption rate that is proportional to the number of both adopters and remaining potential adopters, resulting in an S-shaped logistic curve. This is expected for a process such as vaccine adoption. However, the COVID-19 vaccination rate is constrained by supply on one hand, and hesitancy on the other, in varying capacities across the country, giving rise to different curves, which vary in slope, inflection points and asymptotes from county to county. Therefore, extracting and analyzing characteristics of these curves from

Figure 1 National daily vaccination rate

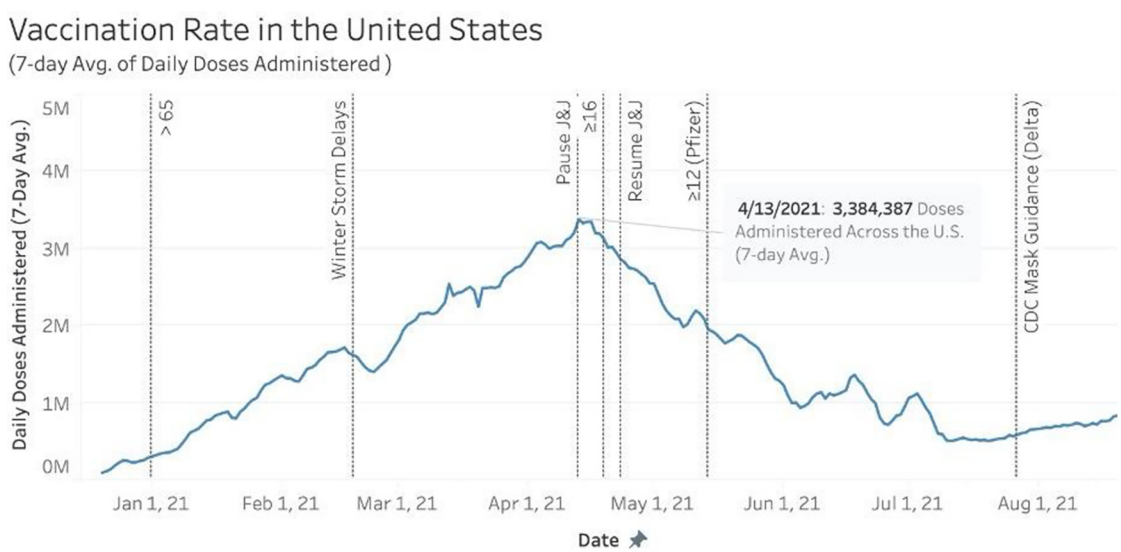

Figure 2 Average county vaccination rates by region, politics and urbanization

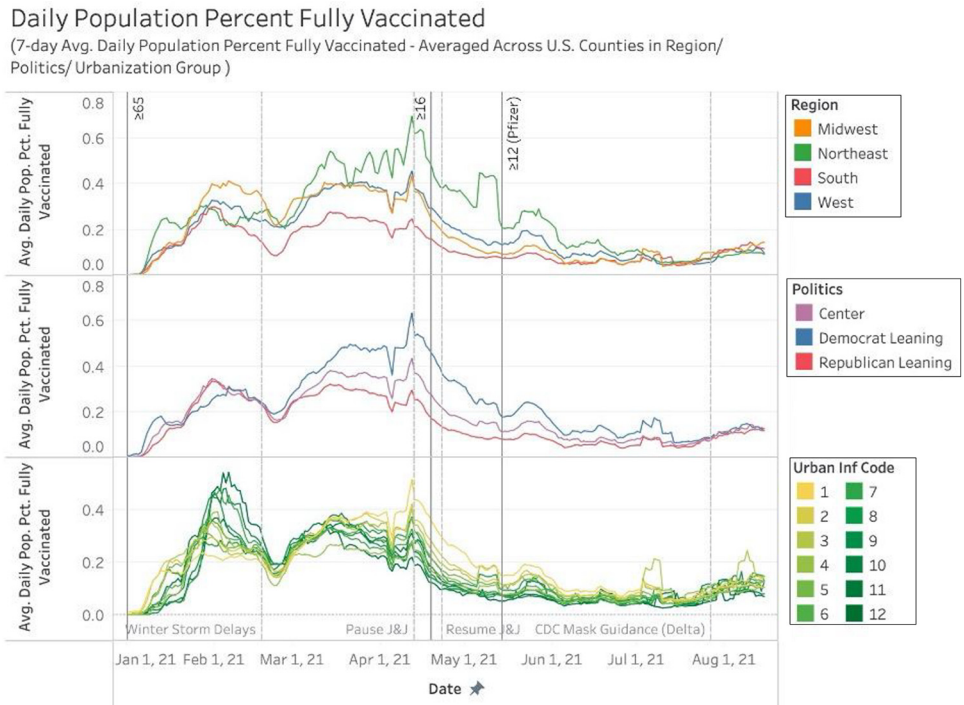

county to county under the two regimes gives insights into how the vaccination distribution process differs across the country.

Each county has a certain maximal vaccination rate, which occurred between the beginning of March and end of April. This peak rate represents the local capacity to administer vaccines, in some instances augmented by resources made available by other jurisdictional levels such as the state or national governments. This interpretation is predicated on the fact, evident in Figure 3, that the vaccine delivery curve (as supplied through the US Federal Government to states and counties) always lies above the cumulative vaccination curve. Considering the cumulative curve, the maximal rate is represented by the maximal tangent slope of the administration curve. After this initial peak, demand for vaccines shrinks and the system transforms into a hesitancy-constrained system, where the capacity to administer doses, or service rate, is now larger than the demand for doses. Identifying this regime requires analysis of a stabilizing slope in the cumulative curve post-April 2021. These supply-constrained and hesitancy-constrained regimes form the focus of the present paper, as the former reflects the inherent ability of the nation in its various jurisdictions to mobilize, while the latter reflects a critical area for public policy to protect the population's overall health and safety.

In the national model of the number of vaccines administered over time, the two-regime framework is characterized by a capacity rate and a hesitancy-constrained demand rate that are tangential to the administration rate curve. Figure 3 illustrates the cumulative number of doses administered and distributed in the USA between December 2020 and September 2021. The curve is smoothed to reflect the 7-day average number of doses. The plot shows the characteristic line for the capacity-constrained and hesitancy-constrained regimes, extracted according to the methodology detailed in the following section.

In the national model, the capacity-constrained regime is characterized by the vaccination rate experienced in mid-April, while the hesitancy-constrained regime is characterized by a stable slope between mid-June and mid-August. The capacity-constrained regime reflects a rate of 3.4 million doses administered per day, while the second regime reflects a hesitancy-constrained demand of 690,000 doses administered per day. The curve for doses distributed closely follows the vaccination rate in April and May, indicating sufficient supply of vaccines, but perhaps insufficient capacity to administer doses.

4.2.1 The supply-constrained regime

The supply-constrained regime is characterized by the maximum vaccination rate experienced in a region. In this paper, the vaccination rate is aggregated up to weekly vaccination figures. The characteristic of the supply-constrained regime is found empirically by taking the maximum slope after buildup has been established, as follows:

$$max(y_{i+1} - y_i) \qquad \forall i \in 1, \ldots, N$$

where:

y_i = cumulative vaccination metric on day/week i (doses administered, population % vaccinated, etc.)

N = the number of days/weeks in the supply constrained regime.

4.2.2 The hesitancy-constrained regime

The hesitancy-constrained regime is characterized by the stabilized slope in the second regime area, which is a direct reflection of the hesitancy-affected demand for vaccination.

Figure 3 Conceptual regime framework (USA National Model)

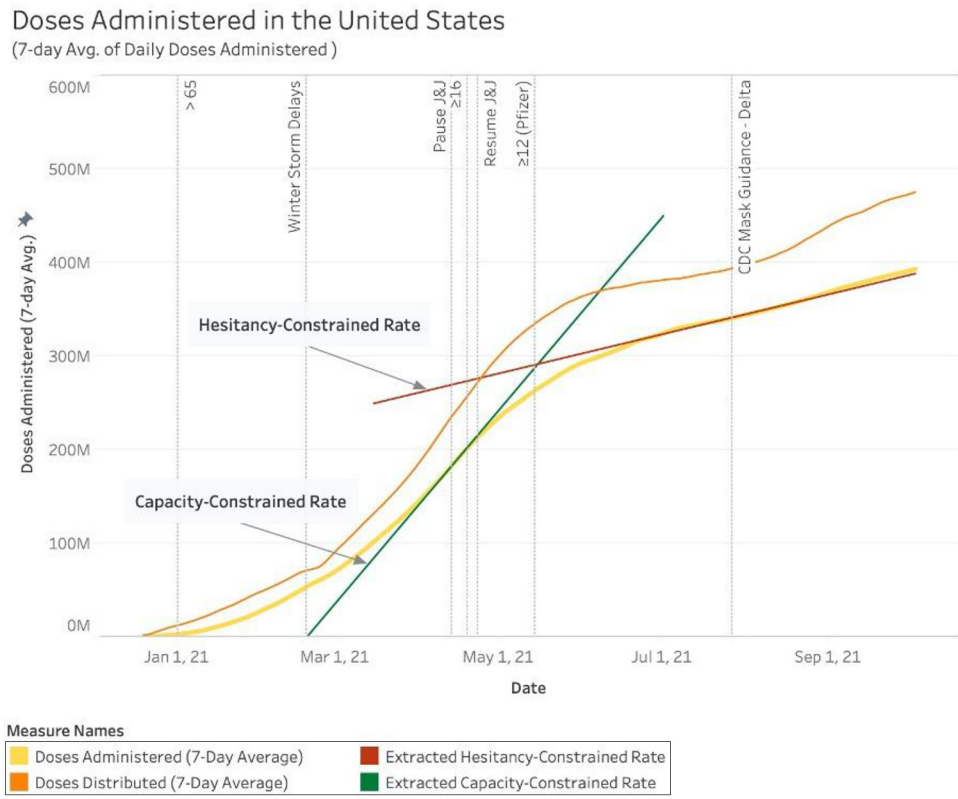

Because of the variation in when this regime starts across regions, the characteristic rate for the hesitancy-constrained demand is determined using a set of three simple linear regression models with time as the independent variable and the vaccination rate as the dependent variable. The first model fits a regression line using the weekly vaccination rates seen between (May 15 and July 15), the second model uses data points from (May 30 to July 30) and the third uses data from (June 15 to July 15). These ranges are identified by visual inspection to reflect most regions. The characteristic rate is found from the following model:

$$vaccination\ rate_i = \beta_0 + \beta_1 \cdot (Week\ Number) + \epsilon_i \; i \in R$$

where:

R = the set of datapoints graphically identified in the hesitancy-constrained regime.

The model with the highest r^2 value is selected and β_1 is taken as the hesitancy-constrained demand rate. For the national model, the r^2 values range from 0.979 to 0.987 with characteristic slopes ranging from 110,000 to 690,000 doses administered per day.

4.3 Analysis method for comparing regime characteristics across counties

To understand how the capacity-constrained vaccination rate and hesitancy-constrained demand for vaccines vary across the country, a simple ordinary least squares (OLS) linear regression model is developed where a set of independent variables, or regressors, are used to explain a relationship with the dependent or response variable, y_i. Each datapoint, i, in the set has a response variable and regressors, $x_i = [x_{i1}, x_{i2}, \ldots, x_{ip}]^T$ and is used to construct a function of the following form:

$$y_i = \beta_0 + \beta_1 x_{i1} + \cdots + \beta_p x_{ip} + \varepsilon_i = x_i^T \beta + \varepsilon_i,$$
$$i = 1, \ldots, n$$

where β_0 is the intercept values and β_k are partial slopes representing the resulting change in y_i for a one unit increase in x_{ik}, when all other regressor values are held constant. In the OLS method, β parameters are chosen to minimize the sum of squared residuals of the model.

5. Results

In this section the extracted rates from analyzing the vaccine rollout across different spatial units are presented first at a state and then county level. The distribution of extracted rates is then presented and the variation in rates is plotted spatially. Finally, multiple regression models are developed to relate these rates to socio-demographic, economic and other indicators.

5.1 Graphical results

Figure 4 depicts the extracted supply-constrained vaccination rate and hesitancy-constrained demand at a state level for the state of California, IL, LA and New Hampshire. These states are selected as they represent each

Figure 4 State-level regime characteristics

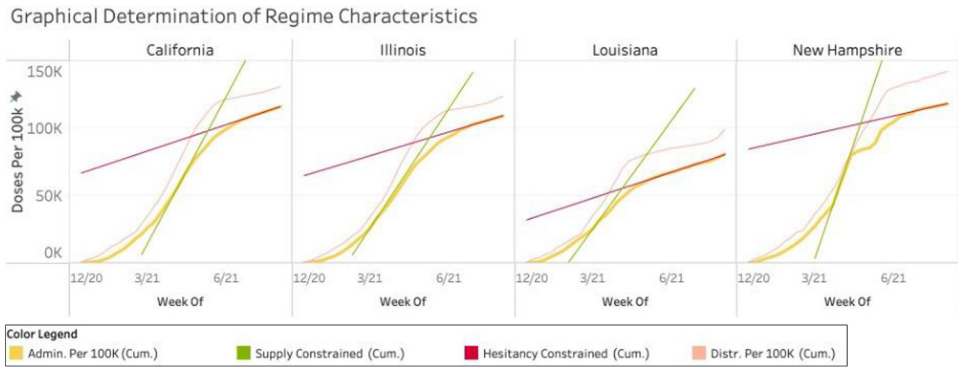

of the four main regional areas in the USA, as well as reflect large-, small- and mid-sized states. The results are presented graphically and are plotted along with the number of doses administered over time, as well as the supply curve of doses delivered to each state.

Figure 4 shows that California, IL, NH and Louisiana administered 8,000, 7,000, 13,000 and 6,000 doses per 100k population at their capacity on 3/28, 3/7, 3/7 and 4/11, respectively. When considering the hesitancy-constrained regime characteristics, the range of demand for vaccines is lower, however, with approximately 1,490, 1,340, 1,460 and 1,020 doses administered per 100k, respectively. New Hampshire, LA and Illinois all reach their vaccination capacity significantly before the peak of the national model in mid-April. California, however, experiences peak vaccination near the peak in the national model. Except for New Hampshire, where the number of distributed doses is close to the vaccine administration rate in mid-April, the distributed doses generally follow the vaccination rate trend for other states. The vaccination rate curve falls below the distribution curve for most states, indicating that the supply-constrained regime is characterized not by a delivery problem, but instead by the actual ability to vaccinate. This indicates a last mile problem as there are doses available to vaccinate at higher rates.

Figure 5 depicts the same extracted supply-constrained vaccination rate and hesitancy-constrained demand at a county level for Cook County, IL, DeKalb County, GA, Los Angeles County, CA, Miami-Dade County, FL and Travis County, TX. These counties are selected as they represent many of the largest metropolitan regions in the USA and cover many of the main U.S. Census Bureau Regions. The plots display the population percent vaccinated in each county over time. Vaccine supply data is not directly available at the county level but can be inferred through tracked vaccination rates. It should be noted that there may be discrepancies in the correlation between the population percent vaccinated and doses administered due to non-adherence to second doses and one dose vaccines. However, this is a reasonable proxy given the available data.

Figure 5 shows that Miami-Dade, DeKalb, Los Angeles, Cook and Travis County administered doses to 4.9, 2.3, 3.8, 4.4 and 5.3% of their populations at capacity during the week of 5/9, 4/18, 4/11, 4/11 and 4/4, but only 1.2, 0.4, 0.7, 1.3 and 0.6% of their populations, respectively, in the hesitancy-constrained regime. Except for Miami-Dade County and Travis County, the peak vaccination rates are experienced near the national model peak in mid-April.

Figure 5 County-level regime characteristics

5.2 Capacity and hesitancy estimations

The two-regime methodology is applied to every county in the USA and analyzed to understand spatial differences across the country in vaccination ability and hesitancy-constrained demand.

Figure 6 displays the distribution of the extracted supply-constrained vaccination rates and hesitancy-constrained demand for vaccines in counties across the USA Outliers are truncated in this graph.

Both distributions of extracted rates follow a bell-shaped curve. The supply-constrained rate peaks with a mean of 3.87% of the population vaccinated per week and a median of 3.62%, with a standard deviation of 2.02%. The distribution of hesitancy-constrained demand rates peaks with a mean of 0.469% of the population vaccinated per week and a median of 0.4%, with a standard deviation of 0.28% Thus, there is variation in the extracted regime characteristic slopes in counties across the nation.

5.2.1 The capacity-constrained regime

Figure 7 maps the variation in capacity-constrained service rates for counties across the continental USA. Counties in red indicate a lower capacity rate for vaccination, whereas counties in green indicate a higher capacity rate for vaccinations. Counties without any color indicate missing or incomplete vaccination data.

Across counties in the USA, there are considerable differences in vaccination rate. Outliers in this graph include counties in Vermont which experienced vaccination rates of over 20% per week. This is likely due to the high demand and small populations present in these counties. Counties in Virginia and Georgia, however, experience rates closer to 1%–2% vaccinated

Figure 6 Histogram of capacity rate and hesitancy-constrained demand across counties

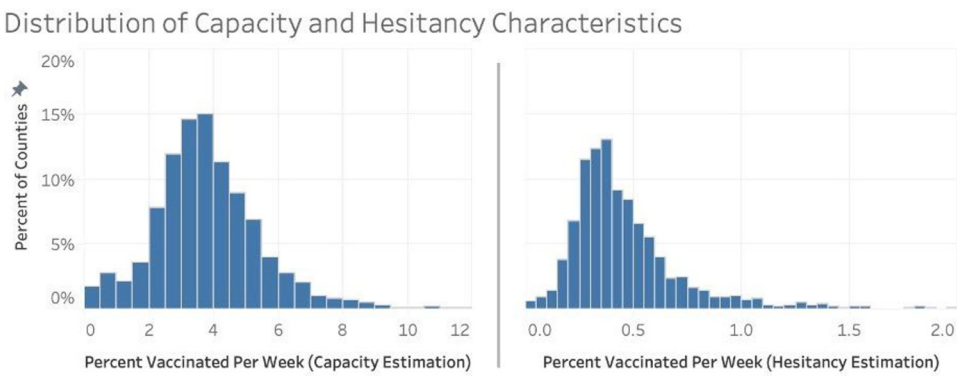

Figure 7 Capacity service rate across counties

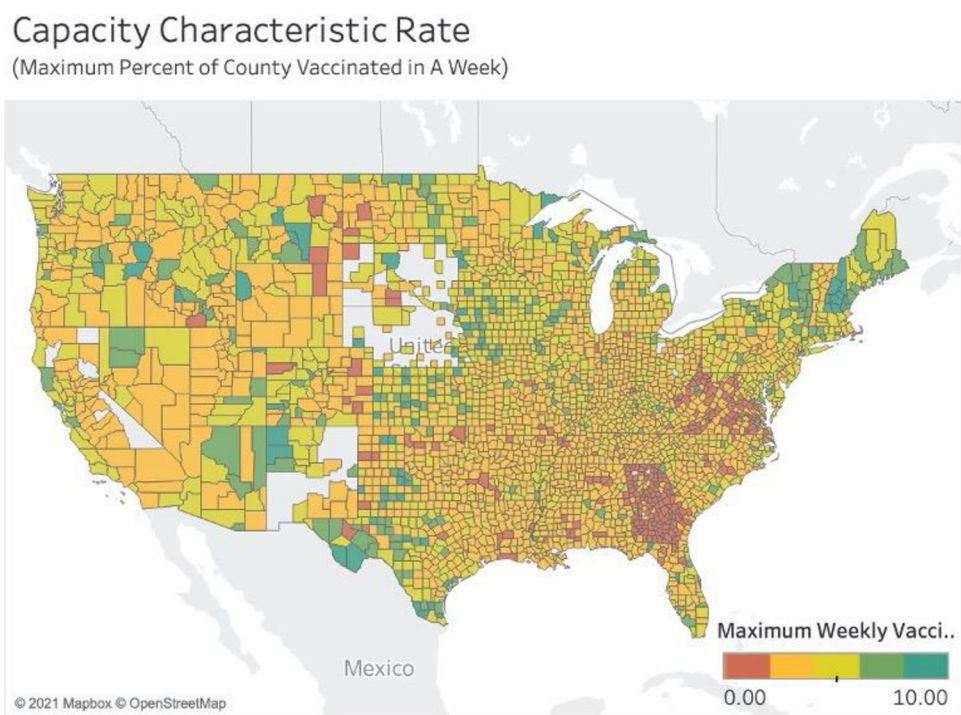

per week, indicating significant regional differences in maximum capacity to vaccinate.

The box plots in Figure 8 further display political variation in capacity rates at a county level. Each boxplot contain datapoints for the extracted capacity regime and the population of the county. The size of each point represents the population size, and major counties are labeled.

As shown in Figure 8, Democratic-leaning counties generally have much higher capacity to vaccinate than those in Center and Republican-leaning counties. The median for Democratic-leaning counties is 4.6%, while the median is 3.7% and 3.5% for Center and Republican-leaning counties. The spread of vaccination rates in Democratic counties ranges across 6.6%, and the range for Center-leaning counties is 7.9% and 6.5% for Republican-leaning counties. The effect of population size on capacity is not particularly evident, as both large and small counties are able to vaccinate at similar rates, indicating population size alone is not a main driver of capacity to vaccinate.

5.2.2 The hesitancy-constrained regime

Figure 9 maps the variation capacity-constrained service rates for counties across the continental USA. Counties in red indicate a lower hesitancy-constrained demand, while counties in green indicate a higher vaccination rate under hesitancy. Counties without any color indicate missing or incomplete vaccination data.

The hesitancy-constrained vaccination demand in Figure 9 varies across the country, however it does not exhibit the exact patterns as the capacity-constrained rate in Figure 7. Many counties experience low vaccination rates in both regimes, indicating an overall lower capacity to vaccinate and low demand for vaccines in the second regime. Counties in the Northeast, however, experience high capacity-rates and low hesitancy-constrained demand. This may indicate an exceeding high initial vaccination level, leaving few unvaccinated to drive the second regime.

The box plots in Figure 10 further display political variation in hesitancy-constrained demand for vaccines at a county level. As in Figure 8, each boxplot contains datapoints for the extracted characteristic slope and population of the county.

As shown in Figure 10, Democratic-leaning counties generally have much higher hesitancy-constrained demand rates that those in Center and Republican-leaning counties. This indicates that the hesitancy-constrained demand for vaccines is higher. The median for Democratic-leaning counties is 0.645%, while the median is 0.42% and 0.38% for Center and Republican-leaning counties. The spread of vaccination rates in Democratic counties ranges 1.4%, and the range for Center-leaning counties is 0.96% and 0.35% for Republican-leaning counties. These indicate a difference in the spread of hesitancy-constrained demand for vaccinations, with a larger variation in rates among Democratic counties. Just as in Figure 8, the effect of population size on demand is not clear as hesitancy-constrained demand for vaccines varies among similar sized counties, indicating population size may not be the main driver of demand under hesitancy.

5.2.3 Relationship between regimes

Figure 11 depicts the relationship between the characteristic slopes of the two regimes. Each data point represents the regime estimates for a single county, the color indicates the

Figure 8 Distribution of county capacity-constrained rates by politics

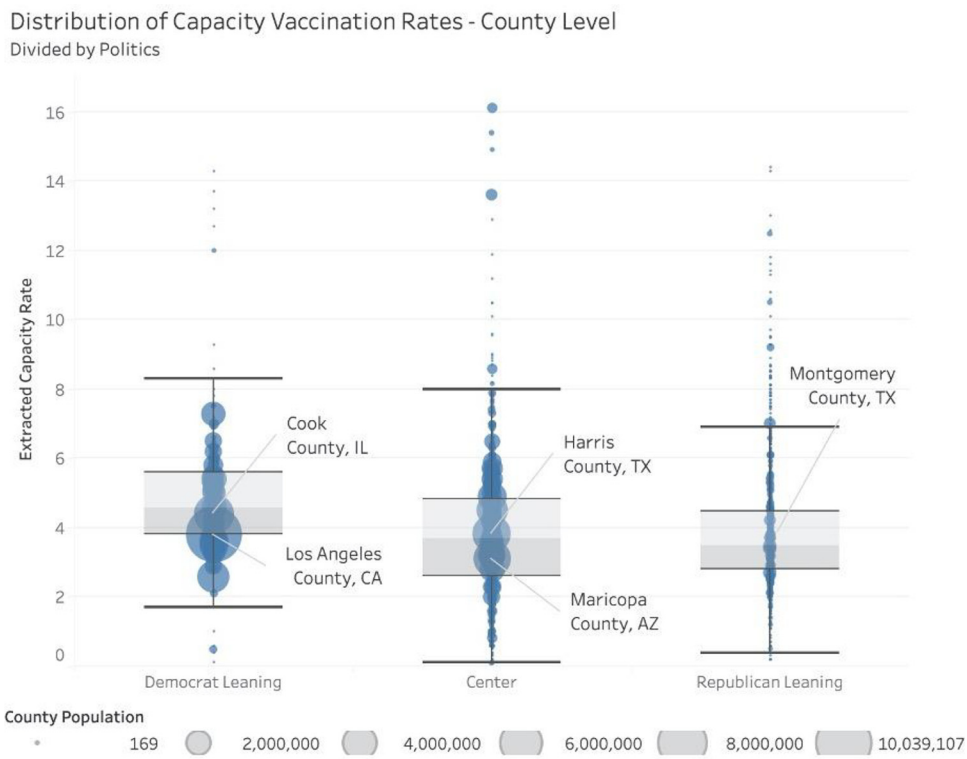

Figure 9 Hesitancy-constrained vaccination rate across counties

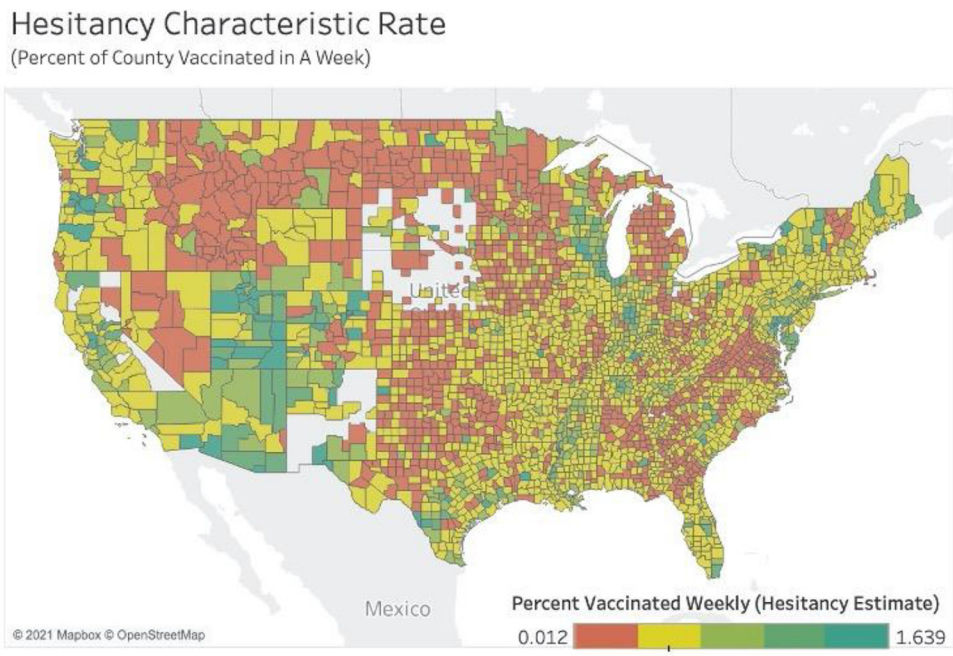

Figure 10 Distribution of county hesitancy-constrained demand by politics

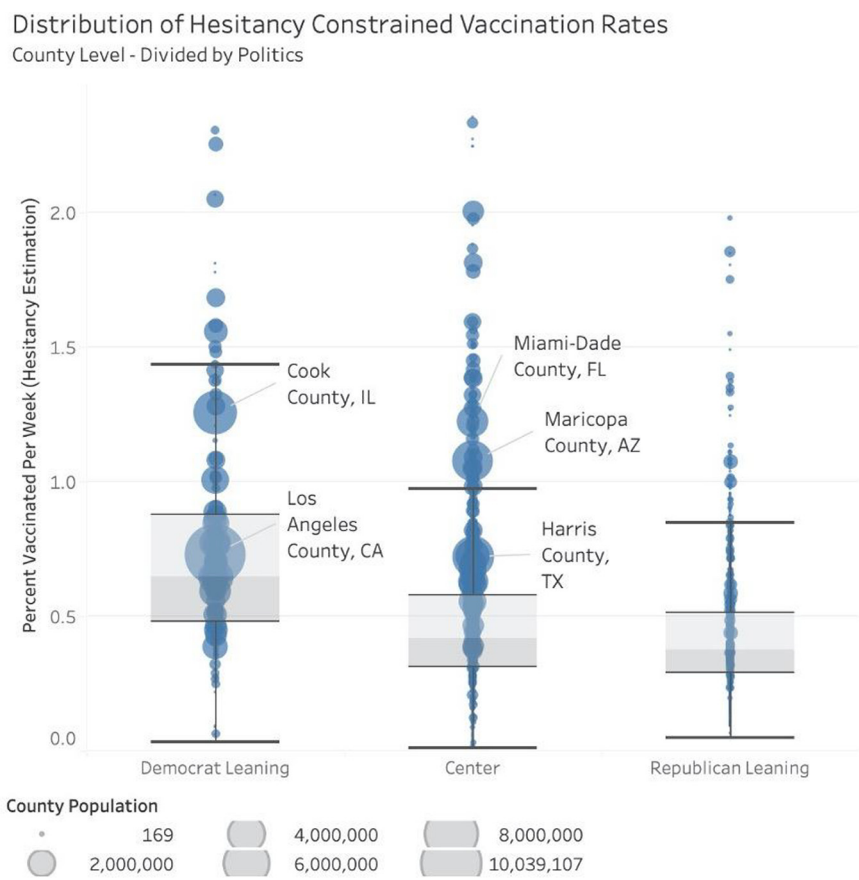

Figure 11 Relationship between hesitancy and capacity-constrained rates

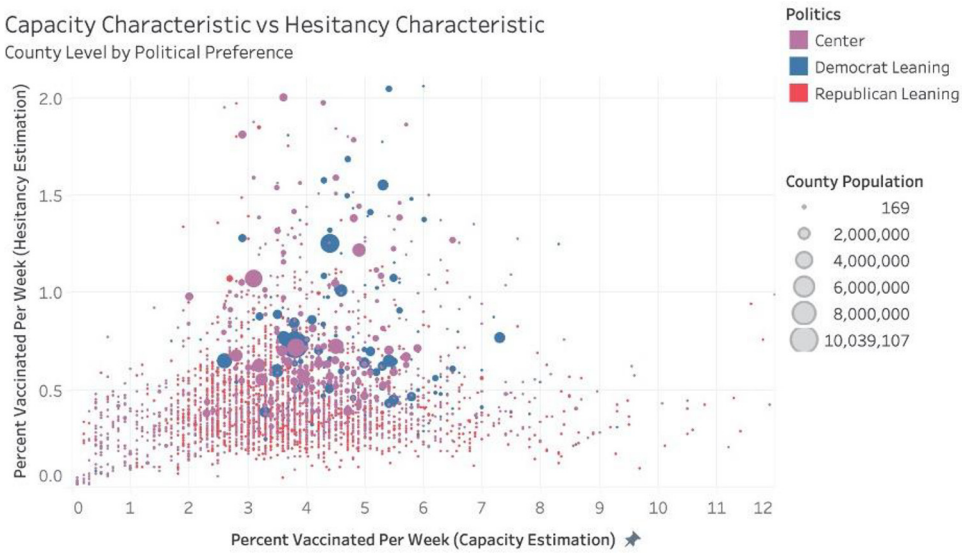

political leaning of the county and the size of the point reflects county population.

Figure 11 shows a slight positive correlation between the rates. Republican-leaning counties tend to have a lower demand for the same capacity estimates.

5.3 Determinants of vaccination capacity and hesitancy-constrained demand

The following section develops multiple linear regression models to understand the various factor affecting two regime characteristics. The models focus on regional, political and urbanization metrics.

5.3.1 Model specification

In this analysis, the exogeneous variables available to us and their sample statistics are as follows:

- Percent Not White/Asian – (Numeric) Percentage of the county not identifying as fully White or Asian. This is used as a metric to understand minority and racial differences. Values range from 1.5 to 100 with a mean of 17.5 and a standard deviation of 17.3.
- Urban Influence Code – (Numeric) County score ranging from 1 to 12, where 1 indicates a county within a large metro area of 1+ million residents and 12 indicates a county that is not adjacent to any metro/micro area and does not contain a town of at least 2,500 residents. Values range from 1 to 12 with a mean of 5.1 and a standard deviation of 3.4.
- Percent Democrat – (Numeric) County percentage voting for the Democratic candidate in the 2020 Presidential Election. Values range from 0 to 0.9 with a mean of 0.3 and a standard deviation of 0.2.
- Democrat Governor – (Binary) Takes a value of 1 if the state's governor identifies as Democratic.
- Region – (Categorical) U.S. Census Bureau Regions: West, Midwest, South and Northeast.

5.3.2 Capacity-constrained vaccination rate model

The final model specification for estimating the capacity-constrained regime vaccination rate is given as follows:

$$\begin{aligned} CapacityRate_i = {} & \beta_0 + \beta_1 \cdot (Region) + \beta_2 \cdot (DemocraticGovernor) \\ & + \beta_3 \cdot (UrbanInfluence) \\ & + \beta_4 \cdot (DemocraticGovernor \cdot UrbanInfluence) \\ & + \beta_5 \cdot (PercentDemocrat) \\ & + \beta_6 \cdot (DemocraticGovernor \cdot PercentDemocrat) \\ & + \beta_5 \cdot (DemocratLeaning) \\ & + \beta_7 \cdot (DemocraticLeaning \cdot PercentNotWhiteAsian) + \epsilon \end{aligned}$$

Table 1 depicts the OLS linear regression results.

The capacity-constrained model confirms the ordering that counties in the Northeast typically experience higher capacity for vaccinations, followed by the Midwest, then the West, and finally the South. Regional and political effects are the most pronounced as a Democratic state governor is expected to increase a county's weekly population vaccinated by 0.54 percentage points. The effect of a unit decrease in urbanization increases a county's vaccination capacity by 0.11 percentage points and this effect is augmented by 0.04% when the county is within a state with a Democratic governor. This indicates that rural counties tend to have higher capacity vaccination rates. This may be due to the sheer size of the population being smaller and more manageable. It may also indicate Democratic governor's push to improve vaccination ability in rural communities. Just as in governor politics, as the percent of Democratic voters increases in a county, the vaccination capacity also increases by 0.6 percentage points. However, the combined effect of a percentage point increase in Democratic voters in a county within a state with a Democratic governor is reduced by 0.03 percentage vaccinated per week at capacity. Finally, in Democratic-leaning counties, the vaccination capacity decreases by 0.02 for each additional population percent that is not White or Asian. This may be indicative of access issues, where race and may play a role in access to

Table 1 OLS Regression results (capacity-constrained)

Regressor	Coefficient	Std err	*t*	P>|*t*|
Intercept	2.00	0.15	13.36	0.00
Northeast	1.11	0.15	7.28	0.00
South	−0.79	0.09	−8.99	0.00
West	−0.20	0.11	−1.89	0.06
Democratic governor	0.54	0.23	2.39	0.02
Urban influence	0.11	0.01	8.61	0.00
Democratic governor – Urban influence	0.04	0.02	1.98	0.05
Percent democrat	0.05	0.00	15.66	0.00
Democratic governor – Percent democrat	−0.03	0.01	−5.90	0.00
Democratic-leaning	0.60	0.09	6.60	0.00
Democratic-leaning – Percent not white/Asian	−0.03	0.00	−9.21	0.00
Dep. variable	Capacity-Constrained Rate		*R-squared*	0.267
Method	OLS		*Adj. R-squared*	0.265

vaccines and vaccination sites. Other races were explicitly tested in this model and were determined insignificant.

5.3.3 Hesitancy-constrained demand model

The final model specification for the estimating the hesitancy-constrained regime vaccination rate is given as follows:

$$\begin{aligned} Hesitancy\,Rate_i = {} & \beta_0 + \beta_1 \cdot (Region) + \beta_2 \cdot (DemocraticGovernor) \\ & + \beta_3 \cdot (UrbanInfluence) \\ & + \beta_4 \cdot (DemocraticGovernor \cdot UrbanInfluence) \\ & + \beta_5 \cdot (PercentDemocrat) + \epsilon \end{aligned}$$

Table 2 depicts the OLS linear regression results.

The hesitancy-constrained model shows regional differences as well; the Midwest has the lowest hesitancy-constrained demand followed by South, Northeast and then the West.

Just as in the model for the capacity-constrained vaccination rate, regional and political effects are the most pronounced. However, a Democratic state governor is expected to decrease a county's hesitancy-constrained demand.

The parameter estimate for urban influence indicates that an increase in United States Department of Agriculture Economic Research Service code, or a decrease in urbanization, reduces the hesitancy-constrained demand. The combined effect of rural areas in states with Democratic governors, however, is a slightly higher demand for vaccines, indicating state leadership has an effect in rural communities. Finally, as the percent of Democratic votes increases by one percentage point in a county, the hesitancy-constrained demand for vaccines increases slightly.

It is of note that the sign for the Democratic governor regressor and urban influence code changes between the two models. This indicates that counties in states with Democratic governors and counties in more rural communities are more likely to have high vaccination capacities, but lower hesitancy-constrained demand for vaccines. This is likely due to the initial push to get vaccinated which is seen in Democratic states where Governors themselves are more likely to reveal that they are vaccinated and encourage others to get vaccinated for economic reopening (Associated Press, 2021), which may have resulted in more resources put in place to vaccinate at higher capacities. Those remaining unvaccinated in these regions likely experience extreme hesitancy and are very unlikely to get vaccinated.

The results of this aggregate cross-sectional study can be used to make broad policy decisions to improve vaccination distribution and availability in the USA. Further behavioral analysis into the mechanisms causing vaccine hesitancy behavior in individuals, however, is needed to develop strong policy solutions and survey-based research may provide more robust insights. Survey studies of vaccine acceptance in the USA, UK and Australia found that, while over 25% of the

Table 2 OLS regression results (hesitancy-constrained)

Regressor	Coefficient	Std err	*t*	P>|*t*|
Intercept	0.3549	0.019	19.055	0
Northeast	0.0328	0.022	1.459	0.145
South	0.0289	0.011	2.536	0.011
West	0.1636	0.015	10.646	0
Democratic governor	−0.1313	0.019	−7.068	0
Urban influence code	−0.0138	0.002	−7.1	0
Democratic governor – Urban influence	0.0059	0.003	2.042	0.041
Percent democrat	0.0064	0	17.683	0
Dep. Variable	Hesitancy-constrained demand		R-squared	0.210
Method	OLS – Least Squares		Adj. R-squared	0.207

population is unwilling to receive vaccines, a majority of this group is not anti-vaccine and may be persuaded through public health initiatives (Trent *et al.*, 2022). Additionally, it was found in New York City and Phoenix that trust and confidence in government was associated with the decision to accept a vaccine. Other survey studies have found that religiosity was negatively correlated with vaccine acceptance (Troiano and Nardi, 2021) and the experience of previous racial discrimination increased hesitancy by 21% (Savoia *et al.*, 2021). Finally, further studies have found increased hesitancy in racial and ethnic minorities (Nguyen *et al.*, 2021).

In conjunction with the findings in this paper, this indicates that American policymakers may want to prioritize increasing vaccine acceptance in counties with lower vaccination percentages as it would provide greater gains toward herd immunity for the country as a whole. The unique polarizing context in the USA requires specific, tailored initiatives across the country. Policy recommendations include countering misinformation through public health communications that are designed around societal and cultural beliefs in individual populations (McAteer *et al.*, 2020). These initiatives should take a community-based approach to identify subpopulations and address their concerns to promote the value of vaccination (Wells *et al.*, 2022).

6. Discussion and conclusion

Considering the COVID-19 vaccine rollout within a multi-regime framework provides insights into a complex system. Characterizing the system by the vaccination rate allows us to evaluate the supply chain and determine potential bottlenecks with only knowledge of the vaccination outcomes at one terminal of the system. The COVID-19 vaccine supply chain exhibits unique dynamics as the extreme demand is initially unserved due to capacity constraints. Within weeks the demand is no longer as intense, and the supply-chain capacity is sufficient. This second regime is characterized by the hesitancy-constrained demand. A multi-regime model allows for the identification of these regimes and frames the end-to-end vaccine supply chain as a dynamic system that experiences constraints on both the supply and demand sides.

From this analysis, it has been shown that the capacity to vaccinate varies significantly across the country by region, politics and demographics. While the national average capacity-constrained rate is 3.4 million doses administered per day (or about 1% of the population vaccinated), the rate varies with 75% of counties experiencing capacity rates between 2% and 5%. From the hesitancy-constrained regime, there is a clear distinction among political lines where Democratic-leaning counties tend to have higher vaccination rates as the hesitancy-constrained demand is higher than in Republican-leaning counties.

Graphical analysis of the two regimes at the state level shows vertical distance between the dose administration rate and the number of doses delivered to the state for most states. This indicates that there is sufficient vaccine supply at the state level and the supply chain is constrained by the ability to vaccinate as opposed to the availability of vaccines. Thus, the supply-constrained regime can be considered a last-mile issue and not a transportation or production issue. The second regime exhibits exclusively last-mile concerns as hesitancy surrounding vaccines drives the lower vaccination rate. Lessons can be extracted from the state-level analysis on the importance of the last-mile operations from a supply and demand perspective in vaccine deployment.

The two-regime framework also helps frame the vaccine rollout within the goal of vaccinating a significant amount of the population. Framing the end-to-end supply chain within these two regimes helps in analyzing and understanding the determinates of low-vaccination rates on the supply and demand side, to understand how these factors are limiting the overall vaccination rates seen across the country. As the demand for booster shots begins to rise, this framework shows that there will not likely be a similar supply-constrained regime as there are many more places to receive the additional dose from as the supply is available. On the demand side, further behavioral survey work is required to develop community-specific plans across the USA to improve vaccination rates.

References

Alam, S.T., Ahmed, S., Ali, S.M., Sarker, S. and Kabir, G. (2021), "Challenges to COVID-19 vaccine supply chain: implications for sustainable development goals", *International Journal of Production Economics*, Vol. 239, p. 108193, doi: 10.1016/J.IJPE.2021.108193.

Associated Press (2021), "Red' states on U.S. electoral map lagging on vaccinations", available at: www.nbcnews.com/politics/politics-news/red-states-u-s-electoral-map-lagging-vaccinations-n1264102 (accessed 7 October 2021).

C, L. and Appa Iyer, S. (2013), "Application of queueing theory in health care: a literature review", *Operations Research for Health Care*, Vol. 2 Nos 1/2, pp. 25-39, doi: 10.1016/j.orhc.2013.03.002.

Centers for Disease Control and Prevention (CDC) (2001), "Update on the supply of tetanus and diphtheria toxoids and of diphtheria and tetanus toxoids and acellular pertussis vaccine", *Journal of the American Medical Association*, Vol. 285 No. 13, p. 1698, doi: 10.1001/JAMA.285.13.1698.

De Boeck, K., Decouttere, C. and Vandaele, N. (2020), "Vaccine distribution chains in low- and Middle-income countries: a literature review", *Omega (United Kingdom)*, Vol. 97, doi: 10.1016/j.omega.2019.08.004.

Duijzer, L.E., van Jaarsveld, W. and Dekker, R. (2018), "Literature review: the vaccine supply chain", *European Journal of Operational Research*, Vol. 268 No. 1, pp. 174-192, doi: 10.1016/J.EJOR.2018.01.015.

Forman, R., Shah, S., Jeurissen, P., Jit, M. and Mossialos, E. (2021), "COVID-19 vaccine challenges: what have we learned so far and what remains to be done?", *Health Policy*, Vol. 125 No. 5, pp. 553-567, doi: 10.1016/j.healthpol.2021.03.013.

Hall, R. (1991), *Queueing Methods: For Services and Manufacturing*, Prentice Hall, Englewood Cliffs, NJ.

Helbing, D. and Lämmer, S. (2005), "Supply and production networks: from the bullwhip effect to business cycles", doi: 10.1142/9789812703248_0002.

Herlin, H. and Pazirandeh, A. (2012), "Nonprofit organizations shaping the market of supplies", *International*

Journal of Production Economics, Vol. 139 No. 2, pp. 411-421, doi: 10.1016/J.IJPE.2011.04.003.

Jacobson, S., Sewell, E., Proano, R., Jacobson, S.H., Sewell, E. C. and Proano, R.A. (2006), "An analysis of the pediatric vaccine supply shortage problem", *Health Care Manage Sci*, Vol. 9, pp. 371-389, doi: 10.1007/s10729-006-0001-5.

Kapadia, A.S., Yu Kun, C. and Kazmi, M.F. (1985), "Finite capacity priority queues with potential health applications", *Computers and Operations Research*, Vol. 12 No. 4, pp. 411-420, doi: 10.1016/0305-0548(85)90038-3.

Kleinrock, L. (1975), "Queueing systems".

Larson, R.C. (1990), "The queue inference engine: deducing queue statistics from transactional data", Vol. 36 No. 5, pp. 586-601, doi: 10.1287/MNSC.36.5.586.

Loomba, S., de Figueiredo, A., Piatek, S.J., de Graaf, K. and Larson, H.J. (2021), "Measuring the impact of COVID-19 vaccine misinformation on vaccination intent in the UK and USA", *Nature Human Behaviour*, Vol. 5 No. 3, pp. 337-348, doi: 10.1038/s41562-021-01056-1.

McAteer, J., Yildirim, I. and Chahroudi, A. (2020), "The VACCINES act: deciphering vaccine hesitancy in the time of COVID-19", *Clinical Infectious Diseases*, Vol. 71 No. 15, pp. 703-705, doi: 10.1093/cid/ciaa433.

Macmillan, C. (2021), "Will you need a COVID-19 booster? What we know so far > news > Yale medicine", available at: www.yalemedicine.org/news/covid-19-booster (accessed 6 October 2021).

MIT Election Data + Science Lab (2021), "County presidential election returns 2000-2020 - U.S. Presidential elections, MIT election data + science lab", available at: www.dataverse.harvard.edu/dataset.xhtml?persistentId=10.7910/DVN/VOQCHQ (accessed 6 October 2021).

Newell, C. (2013), *Applications of Queueing Theory*, Springer Science\& Business Media.

Newell, G.F. (1993), "A simplified theory of kinematic waves in highway traffic, part II: queueing at freeway bottlenecks", *Transportation Research Part B: Methodological*, Vol. 27 No. 4, pp. 289-303, doi: 10.1016/0191-2615(93)90039-D.

Nguyen, L.H., Joshi, A.D., Drew, D.A., Merino, J., Ma, W., Lo, C.H., Kwon, S., Wang, K., Graham, M.S., Polidori, L. and Menni, C. (2021), "Racial and ethnic differences in COVID-19 vaccine hesitancy and uptake", *Preprint. Epidemiology*, doi: 10.1101/2021.02.25.21252402.

Nirappil, F., Goldstein, A. and Beachum, L. (2021), "Storm delays 6 million coronavirus vaccine doses, white house announces – The Washington Post, Washington post", available at: www.washingtonpost.com/health/2021/02/19/vaccines-delayed-winter-storm/ (accessed 6 October 2021).

Roozenbeek, J., Schneider, C.R., Dryhurst, S., Kerr, J., Freeman, A.L., Recchia, G., Van Der Bles, A.M. and Van Der Linden, S. (2020), "Susceptibility to misinformation about COVID-19 around the world", *Royal Society Open Science*, Vol. 7 No. 10, doi: 10.1098/RSOS.201199.

Savoia, E., Piltch-Loeb, R., Goldberg, B., Miller-Idriss, C., Hughes, B., Montrond, A., Kayyem, J. and Testa, M.A. (2021), "Predictors of COVID-19 vaccine hesitancy: socio-demographics, co-morbidity, and past experience of racial discrimination", *Vaccines*, Vol. 9 No. 7, doi: 10.3390/vaccines9070767.

Singer (2021), "Where do vaccine doses go, and who gets them? The algorithms decide – The New York Times, New York Times", available at: www.nytimes.com/2021/02/07/technology/vaccine-algorithms.html (accessed 6 October 2021).

Texas DSHS (2021), "COVID-19 vaccine allocations, department of state health services", available at: www.dshs.texas.gov/coronavirus/immunize/vaccineallocations.aspx (accessed 6 October 2021).

Trent, M., Seale, H., Chughtai, A.A., Salmon, D. and MacIntyre, C.R. (2022), "Trust in government, intention to vaccinate and COVID-19 vaccine hesitancy: a comparative survey of five large cities in the United States, United Kingdom, and Australia", *Vaccine*, Vol. 40 No. 17, pp. 2498-2505, doi: 10.1016/j.vaccine.2021.06.048.

Troiano, G. and Nardi, A. (2021), "Vaccine hesitancy in the era of COVID-19", *Public Health*, Vol. 194, pp. 245-251, doi: 10.1016/j.puhe.2021.02.025.

U.S. Census Bureau (1984), "U.S. Census Bureau – Census regions and divisions of the United States, U.S. Census Bureau", available at: www.www2.census.gov/geo/pdfs/maps-data/maps/reference/us_regdiv.pdf (accessed 6 October 2021).

U.S. Census Bureau (2019), "County population by characteristics: 2010-2019", available at: www.census.gov/data/tables/time-series/demo/popest/2010s-counties-detail.html (accessed 7 October 2021).

USDA ERS (2013), "USDA ERS – Urban influence codes, U.S. Department of agriculture", available at: www.ers.usda.gov/data-products/urban-influence-codes/ (accessed 6 October 2021).

Wells, K., Moore, K.L. and Bednarczyk, R. (2022), "Supporting immunization programs to address COVID-19 vaccine hesitancy: recommendations for national and community-based stakeholders", *Vaccine [Preprint]*.

Corresponding author

Karen Smilowitz can be contacted at: ksmilowitz@northwestern.edu